Research Square

Preprints are preliminary reports that have not undergone peer review.
They should not be considered conclusive, used to inform clinical practice,
or referenced by the media as validated information.

Regional Cerebral Blood Flow Is Reduced in Older Adults with Type 2 Diabetes and Obesity and Is Associated with Cognitive Function and Metabolic Dysfunction

Mohamad Elsharydah
The University of Texas Southwestern Medical Center
Jeff Schaffert
The University of Texas Southwestern Medical Center
Anujit Saha
The University of Texas Southwestern Medical Center
Jack Kaufman
The University of Texas Southwestern Medical Center
Jennine Leary
The University of Texas Southwestern Medical Center
Alison Jin
The University of Texas Southwestern Medical Center
Jaime Almandoz
The University of Texas Southwestern Medical Center
Binu Thomas
binu.thomas@utsouthwestern.edu

The University of Texas Southwestern Medical Center

Article

Keywords: 1. Type 2 Diabetes, 2. Obesity, 3. Older adults, 4. Cerebral blood flow (CBF), 5. Cognitive function

Posted Date: November 19th, 2026

DOI: https://doi.org/10.21203/rs.3.rs-10569496/v1

License: This work is licensed under a Creative Commons Attribution 4.0 International License.
Read Full License

Additional Declarations: No competing interests reported.

Abstract

Type 2 diabetes (T2D) and obesity in older adults are established risk factors for Alzheimer's disease and related dementia (ADRD), yet the mechanisms linking these conditions to cognitive decline remain incompletely understood. Arterial spin labeling (ASL) perfusion MRI provides a noninvasive approach for exploring the vascular processes underlying early cognitive decline. Few studies have integrated ASL methods with comprehensive neuropsychological testing, systemic blood markers, and structural analysis in this population.

In this exploratory pilot study, voxel-based analysis ($p < 0.001$; cluster size ≥ 10 voxels) revealed that older adults with T2D and obesity (N = 14; median BMI, 32.74 kg/m^2 [IQR, 31.2–34.2]; range, 30.5–41.5) showed approximately 37% lower cerebral blood flow (CBF) in posterior brain regions, mainly the bilateral occipital cortex, compared with age- and sex-matched controls. The bilateral occipital cluster remained significant after FWE correction ($p = 0.020$). The T2D and obesity group also exhibited lower performance on the Repeatable Battery for the Assessment of Neuropsychological Status (RBANS) attention ($p = 0.035$) and global cognition ($p = 0.022$) indices, as well as lower Delis-Kaplan Executive Function System (D-KEFS) Color-Word switching ($p = 0.001$) scores. Across all participants, lower CBF was associated with higher HbA1c ($p = 0.003$) and greater insulin resistance ($p = 0.008$), whereas higher CBF was associated with better global cognitive performance ($p = 0.003$).

Regional hypoperfusion in people with T2D and obesity was associated with poorer metabolic markers (e.g., HbA1c, fasting glucose) and lower cognitive performance, in the absence of structural differences. These findings may suggest that cerebral perfusion may reflect an early vascular or metabolic correlate of cognitive vulnerability that could precede overt clinical impairment, but confirmation is needed in larger, more controlled longitudinal studies.

Introduction

The prevalence and incidence of type 2 diabetes (T2D) has increased markedly worldwide over the last three decades [1]. Older adults are particularly at risk, with the global T2D prevalence exceeding 20% per 5-year age strata between 65 and 95 years old [2]. Long-term macrovascular (e.g., atherosclerosis) and microvascular complications (e.g., retinopathy, nephropathy) contribute substantially to overall morbidity and mortality in older adults with T2D [3]. However, the impact of T2D on cognitive status and decline is less frequently emphasized. A growing body of evidence demonstrates that T2D is a risk factor for Alzheimer’s disease and related dementia (ADRD), with reported hazard ratios approaching 2.0 [4–7].

T2D and ADRD share overlapping pathophysiological pathways, including insulin resistance, cerebrovascular dysfunction, dyslipidemia, amyloid deposition, neuroinflammation, and impaired mitochondrial and synaptic function, suggesting that targeting metabolic and vascular risk factors may prevent or delay cognitive decline [8–11]. Despite these shared mechanisms, the biological link between T2D and ADRD pathology remains incompletely understood [8, 9, 12]. Obesity can further compound this

relationship. Not only is midlife obesity a catalyst for T2D pathogenesis [13], but it also serves as an independent risk factor for ADRD [14]. In late life, however, obesity plays a more complex role, with some studies reporting that obesity is associated with lower ADRD risk [15], a phenomenon often referred to as the “obesity paradox” [15]. Findings regarding obesity and cognition in individuals with T2D have likewise been mixed, with studies reporting positive, negative, or no associations between BMI and cognitive performance [16–18]. These discrepancies suggest that the relationship between obesity and cognitive function is subtle and influenced by factors such as age, adiposity distribution, cardiovascular comorbidity, frailty, metabolic reserve, and socioeconomic status [18–21]. Although substantial evidence links T2D to poorer cognitive performance and increased dementia risk [20], the contribution of obesity to cognitive outcomes in individuals with T2D remains less clear. Obesity itself has been associated with cerebral small vessel disease, brain atrophy, reduced hippocampal and hypothalamic integrity, diminished vascular and cognitive function [22–25]. Together, T2D and obesity may exert additive or synergistic effects on cerebrovascular and metabolic dysfunction, impairing cerebral perfusion and metabolic efficiency and thereby increasing vulnerability to cognitive decline. Additionally, while obesity commonly co-occurs with T2D, cerebrovascular status in individuals with both conditions remains comparatively understudied. These inconsistencies highlight the need to further characterize cerebrovascular and cognitive health in populations with coexisting T2D and obesity.

Perfusion imaging offers one mechanistic window into this relationship, enabling direct evaluation of the cerebrovascular dysfunction implicated in both T2D and ADRD. Arterial spin labeling (ASL) MRI has been used to study perfusion noninvasively for over three decades, without the need for exogenous contrast agents or radioactive materials [26]. ASL has broad clinical and translational utility, especially in stroke [27], neuro-oncology [28], aging [29], mild cognitive impairment [30], dementia [31], migraine [32], traumatic brain injury [33], exercise interventions [34–36], and as a biomarker to predict cognitive function in older adults [37]. Although several published studies have explored ASL-derived blood flow differences in T2D, the methods and results remain highly heterogenous. Studies have reported hypoperfusion in regions across the cortices, whereas others, especially in diabetic retinopathy, have reported a paradoxical increase in perfusion in T2D patients compared with controls [38–42]. These heterogeneous results make it difficult to fully understand the impact of T2D on cerebrovascular function and may limit the translational and clinical utility of ASL in this population.

To date, T2D with an obesity phenotype remains understudied in ASL-MRI, and ASL acquisitions adhering to the White Paper recommendations [31] are largely absent from T2D cohort studies. Furthermore, many authors do not implement comprehensive cognitive testing, instead, they rely on cognitive screening tools, such as the MMSE or MoCA, or on isolated domain-specific tests [40, 43–45]. Thus, subtle cognitive deficits may not have been detected in participants without mild cognitive impairment (MCI) or dementia. Similarly, blood-based biomarkers of metabolic dysfunction (e.g., hemoglobin A1c, insulin resistance, adipokines) are absent from many ASL T2D studies. Because brain function is associated with systemic pathology (e.g., poor glycemic control) [46, 47], the inclusion of blood biomarkers would be important in understanding the processes underlying cognitive decline in people with T2D. Prior ASL studies in T2D have primarily focused on cerebral perfusion and cognition, whereas

comparatively few investigations have integrated ASL-derived perfusion measures with comprehensive neuropsychological testing, systemic blood biomarkers, and structural brain imaging in the same participants [48, 49].

In this pilot study, we aimed to use the three-dimensional (3D) pCASL technique to investigate whether regional perfusion differences exist between older adults with T2D and obesity (T2D+Obesity), and between age- and sex-matched participants without T2D or obesity (controls). We also implemented a comprehensive neuropsychological battery to detect even subtle differences in neurocognitive function. Systemic markers of T2D including glycemic markers, insulin, lipids, and adipokines, were also collected. We hypothesized that perfusion would be significantly lower in older adults with T2D+Obesity compared to controls. We also hypothesized that blood markers indicative of poor glycemic control are associated with poor cerebral perfusion, and that poor cerebral perfusion is associated with lower cognitive performance, which is consistent with an increased risk for ADRD.

Methods

Participants and Inclusion and Exclusion Criteria

This was a cross-sectional, observational pilot study approved by the University of Texas Southwestern (UTSW) Medical Center (Dallas, Texas, United States of America) Institutional Review Board and conducted from December 2023 to February 2026. Participants were recruited from UTSW general internal medicine clinics with messages sent through the electronic patient portal. All participants provided written informed consent to participate.

The following criteria were applied to all participants: (1) Age 55–85 years; and (2) English language proficiency sufficient for study participation.

The inclusion criteria for older adults with T2D+Obesity were as follows: (1) Clinical diagnosis of T2D or taking medications for T2D; (2) Hemoglobin A1c (HbA1c) blood level of 6.0–10% within the past 6 months; and (3) BMI of 30–45 kg/m^2.

The inclusion criteria for control participants were as follows: (1) BMI = 22.5–27.5 kg/m^2; (2) HbA1c level of less than 5.7% within the past 6 months; and (3) controlled hypertension (systolic blood pressure of < 140 and diastolic blood pressure of < 90).

The exclusion criteria for all participants were as follows: (1) body weight > 450 lbs; (2) contraindications to MRI (e.g., metallic implants, non-removable piercings, or claustrophobia); (3) major pre-existing neurological disorders (including stroke, transient ischemic attack, and neurocognitive disorders); (4) psychiatric disorders (e.g., psychosis, bipolar disorder, major depression), (5) prior heart disease (e.g., arrhythmia, coronary artery disease, pericarditis, or angina); (6) prior bariatric surgery; (7) weight loss > 5% within the preceding 6 months; (8) current smoking or recreational drug use; (9) chronic kidney

disease stage 4–5, end-stage kidney disease, or prior kidney transplantation; (10) pre-menopausal status; and (11) clinically significant age-related hearing loss.

Clinical and Laboratory Measurements

A complete medical and surgical history, anthropometric data (weight, height, and waist circumference), and vital signs (heart rate, and blood pressure) were collected at the initial screening visit. If recent (< 6 months) HbA1c data were not available in the medical records, a blood draw for HbA1c was performed to assess whether the participant met the inclusion criterion.

At the study visit, a blood was drawn from each participant after overnight fasting. Blood markers, including a comprehensive metabolic panel (CMP), lipid profile, insulin, and adipokines were processed externally by Quest Diagnostics Inc. (Secaucus, New Jersey, USA). Blood markers, including HbA1c, collected at this imaging visit were used for reporting and analysis here. Insulin resistance was calculated using the homeostasis model assessment of insulin resistance (HOMA-IR) method [50].

MRI experiments and imaging parameters

MRI scans were performed on a 3T Siemens MAGNETOM Prisma scanner (Erlangen, Germany). A 64-channel head coil was used for signal reception. During scanning, the participants were instructed to relax and to not think of anything particularly.

For cerebral blood flow (CBF) assessment, a single-delay 3D gradient and spin-echo (GRASE) pCASL scan was acquired with 32 slices covering the entire brain using the following parameters: isotropic voxel size = 3.5 mm, TR = 4330 ms, TE = 31.68 ms, FOV = 224 mm, phase FOV = 100%, flip angle = 120°, label duration = 1800 ms, post-label delay (PLD) = 2000 ms. This PLD is consistent with recommendations for older adults and clinical patients [31]. Images were acquired with fat saturation. A separate proton density calibration image was acquired for CBF quantification. The pCASL sequence was implemented using ASL software provided by the Stevens Neuroimaging and Informatics Institute at the University of Southern California [51].

For structural assessment, a 3D T1-weighted multi-echo magnetization-prepared rapid gradient echo (MEMPRAGE) acquisition was performed with 176 sagittal slices using the following parameters: isotropic voxel size = 1.0 mm, TR = 2530 ms, TI = 1100 ms, FOV = 256 mm, matrix = 256 × 256, phase FOV = 100%, flip angle = 7°, and four echo times (TE = 1.69, 3.55, 5.41, and 7.27 ms). Parallel imaging was applied using GRAPPA with an acceleration factor of 2 in the phase-encoding direction. A root mean square averaged image was generated by the scanner from the four acquired echoes, which was used for further processing. The MEMPRAGE image provides significantly lower B0-related distortion and enhanced cortical segmentation accuracy over the typical single echo MPRAGE image.

Image processing

pCASL images were converted to 4D ANALYZE format prior to processing via the ASL-MRICloud pipeline (https://braingps.mricloud.org/asl) [52]. Within ASL-MRICloud, motion correction was performed, and the signal difference between the control and label image pairs (control – label) was calculated. Voxel-wise absolute CBF was calculated using the following equation [52]:

$$f = \frac{6000 * \lambda \, \Delta \, M * e^{PLD \cdot \, R_{1a}}}{2\alpha * T_{1a} * M_0 * (1 - e^{-\tau \, \cdot \, R_{1a}})}$$

where *f* represents CBF in mL/100 g/min, ΔM represents the difference in signal intensity between the control and label images, M_0 represents equilibrium longitudinal magnetization (derived from the calibration image), $R_{1a} = 1/T_{1a}$ represents the longitudinal relaxation rate of arterial blood in Hz (where T_{1a} is assumed to be 1650 ms), and τ represents the labeling duration (1800 ms) [52]. The PLD, as described previously, was 2000 ms. Other assumptions for CBF quantification included a brain/blood partition coefficient (λ) = 0.9 ml/g and labeling efficiency (α) = 0.85.

T1-weighted image processing was performed using CAT12 [53] within Statistical Parametric Mapping (SPM25, Wellcome Centre for Human Neuroimaging), running in MATLAB (MathWorks, Natick, MA). For each participant, a modified T1-weighted (bias, intensity, and noise corrected) image was generated, followed by skull-stripping to remove non-brain tissue and improve spatial registration quality. The processed T1-weighted image then served as an anatomic reference in a two-step registration procedure in SPM25 to transform each pCASL image into standard MNI space.

The resulting CBF maps were visually inspected for artifacts. Spatial smoothing was then applied using an isotropic Gaussian kernel with an 8.75 mm full width at half maximum (FWHM) in SPM25.

MEMPRAGE images were additionally processed using FreeSurfer's recon-all pipeline (version 8.1.0; https://surfer.nmr.mgh.harvard.edu/) to derive regional volume and cortical thickness measurements. Regional volumes were normalized to estimated total intracranial volume (eTIV). Finally, white matter hyperintensity (WMH) volumes were derived from CAT12 segmentation and normalized.

Neuropsychological assessment

Neuropsychological assessment was performed on the same day as the imaging visit by an experienced clinical neuropsychologist or psychometrician under neuropsychologist supervision at the UTSW. The cognitive domains of immediate memory, delayed memory, visuospatial ability, language, and attention were assessed using the Repeatable Battery for the Assessment of Neuropsychological Status (RBANS) [54]. Individual RBANS subtest scores are reported, as are indices of attention/processing speed, language, visuospatial skills, and memory, along with a global cognitive composite derived from these domains. Processing speed and executive function were further assessed using the Trail Making Test

(TMT) Part A and B [55] and the Texas Card Sorting Test (TCST) Logical Sorts subtest [56]. Additional measures of executive functioning included the Color and Word Interference Test (CWIT) from the Delis-Kaplan Executive Function System (D-KEFS), which provides measures of speeded word and color naming, the Stroop inhibition effect, and switching/mental flexibility [57].

Statistical analysis

CBF Maps

Statistical analysis of the voxel-wise absolute CBF maps was performed in SPM25. Voxel-wise group comparisons were conducted using a two-sample t-test within the general linear model framework, with age and sex included as covariates of no interest. Both contrasts (controls > T2D+Obesity and T2D+Obesity > controls) were evaluated.

Statistical t-test maps were thresholded at an uncorrected voxel-wise significance level of $p < 0.001$ with a cluster extent threshold of 10 contiguous voxels. Because the voxel-wise CBF comparison represented the primary imaging analysis, clusters surviving FWE correction were considered corrected primary findings. An additional intensity threshold of 5 ml/100g/min was applied to exclude physiologically implausible values, as perfusion at these levels would be incompatible with tissue viability and is likely due to partial volume effects or smoothing artifacts. The peak MNI coordinates from each significant cluster were then entered into a Python-based lookup tool (https://github.com/tsbinns/mni_to_atlas) to derive anatomical region of interest (ROI) labels based on the Automated Anatomical Labelling 3 (AAL3) atlas [58].

Clinical, neuropsychological, and structural data

Statistical analyses of the clinical, neuropsychological, and structural measures were performed in R (RStudio, version 2025.09.2). For continuous clinical variables, group differences between T2D+Obesity participants and control participants were assessed with Welch's two-sample t-test. Neuropsychological outcomes are reported as norm-adjusted percentile scores, which are bounded and rank-based; accordingly, between-group differences were assessed using Mann-Whitney *U* tests. Categorical variables were assessed with Fisher's exact test. Effect sizes for continuous clinical variables were reported as Hedges' *g* (T2D+Obesity – controls), rank-biserial correlations were reported for neuropsychological outcomes, and odds ratios were reported for categorical variables.

The RBANS, D-KEFS and TCST Logical Sorts scores were age-adjusted according to standardized testing procedures (i.e., RBANS, D-KEFS, and TCST manual normative data) prior to statistical analysis [56]. TMT Part A and TMT Part B were norm-referenced to age, sex, race, and education (i.e., Heaton norms) [59].

Following normalization to eTIV, structural data analysis was restricted to ROIs overlapping with significant clusters identified in the SPM25 voxel-wise analysis. Group differences were assessed using

linear regression models with group as the predictor of interest and sex and age included as covariates. Standardized β coefficients are reported.

Notably, *p*-values < 0.05 were considered significant given the limited sample size and exploratory nature of this study. No adjustment for multiple comparisons was applied.

Association analyses

Association analyses were performed between CBF and continuous clinical variables that demonstrated significant ($p < 0.05$) group differences. CBF for each participant was derived by averaging voxel-wise CBF values across all significant clusters (combined cluster CBF) identified in the voxel-wise SPM25 group comparison analysis. These combined cluster CBF values were extracted without prior covariate adjustment. Participants with missing data for a given variable were excluded from the corresponding model.

First, associations between combined cluster CBF and blood markers were assessed using multivariable linear regression models with combined cluster CBF as the dependent variable and each blood marker entered separately as the predictor of interest, with age and sex included as covariates. Adjusted R^2 values and covariate-adjusted *p*-values are reported in the corresponding plots. Second, associations between combined cluster CBF and neuropsychological measures were explored. For these analyses, CBF values were first residualized for the same demographic variable(s) used in the normative adjustment of each neuropsychological outcome (i.e., because RBANS scores are age-normed, age-residualized CBF values were used). Correlation analyses were then performed between the residualized CBF values and the corresponding neuropsychological outcomes, with Pearson correlation coefficients (r) and *p*-values reported. Statistical significance was defined as $p < 0.05$. Because these analyses were secondary and exploratory, effect estimates and nominal *p*-values are reported and interpreted as hypothesis-generating rather than confirmatory. No adjustment for multiple comparisons was applied.

Results

Demographic and clinical characteristics of the participants

In total, 32 age and sex-matched participants were enrolled in this pilot study and were grouped into either the T2D+Obesity group or the control group. Demographic and clinical markers of the participants are presented in Table 1. Age, sex distribution, and years of education did not differ between groups (all $p > 0.05$). BMI and the waist-to-height ratio, a measure of central adiposity, were significantly higher in those with T2D+Obesity (all $p < 0.001$). Markers of glycemia and insulin resistance, including HbA1c, fasting plasma glucose, peripheral blood insulin, and HOMA-IR were also significantly elevated in participants with T2D+Obesity (all $p < 0.05$). Among blood lipid measures, total cholesterol, LDL, and HDL

were significantly greater in control participants (all $p < 0.05$). Leptin and adiponectin were also significantly different between the groups (all $p < 0.05$).

Table 1

Basic demographic information and relevant clinical markers in all participants. Values are given as mean ± SD, male/female counts (n/n), n (%), or N/A. A value of 12 years for education indicates high school graduate or equivalent GED. Group comparisons were performed using Welch's t-test. Fisher's exact test was used to compare categorical variables.

Basic demographics	**T2D+Obesity (*N* = 14)**	**Controls (*N* = 18)**	***p* value**	**Effect size[c]**
Age (years)	70 ± 6.1	68 ± 7.9	0.483	0.239
Sex (male/female)	7/7	8/10	1.000	0.806
Education (years)	15 ± 3.4	16.5 ± 2.3	0.214	-0.466
Anthropometrics				
BMI (kg/m^2)	34 ± 3.3	25 ± 2.4	< 0.001*	3.14
Waist/height ratio (a.u.)	0.67 ± 0.061	0.52 ± 0.053	< 0.001*	2.59
Diabetes markers				
Duration of T2D (years)[a]	5.71 ± 4.8	N/A	N/A	N/A
HbA1c (%)	6.7 ± 0.69	5.6 ± 0.27	< 0.001*	2.30
FPG (mg/dL)	125 ± 20	92 ± 8.6	< 0.001*	2.19
Insulin (uIU/mL)	18.3 ± 9.3	9.7 ± 7.5	0.009*	1.01
HOMA-IR (a.u.)	5.6 ± 2.9	2.2 ± 1.8	< 0.001*	1.43
Blood pressure				
Systolic (mmHg)	134 ± 19	127 ± 12.0	0.210	0.476
Diastolic (mmHg)	79 ± 8.3	76 ± 7.9	0.283	0.383
MAP (mmHg)	97 ± 11	93 ± 8.0	0.185	0.491
Lipids				
Total cholesterol (mg/dL)	152 ± 35	192 ± 45	0.009*	-0.946
HDL (mg/dL)	47 ± 7.6	62 ± 16	0.001*	-1.15
Triglycerides (mg/dL)	151 ± 74	106 ± 59	0.073	0.670
LDL (mg/dL)[b]	81 ± 28	109 ± 35	0.017*	-0.855
Non-HDL (mg/dL)[b]	105 ± 32	130 ± 37	0.054	-0.683

Basic demographics	T2D+Obesity (*N* = 14)	Controls (*N* = 18)	*p* value	Effect size[c]
Adipokines				
Adiponectin (ug/mL)	9.3 ± 4.2	16 ± 9.3	0.010*	-0.921
Leptin (ng/mL)	14 ± 8.5	5.2 ± 4.6	0.003*	1.25
IL-6 (pg/mL)	4.14 ± 2.44	4.34 ± 5.51	0.888	-0.045
Medications				
Metformin use, n (%)	11 (79%)	0 (0%)	< 0.001*	N/A
Statin use, n (%)	10 (71%)	8 (44%)	0.165	3.01
Anti-hypertensive use, n (%)	12 (86%)	4 (22%)	< 0.001*	18.4
[a] Duration obtained from what was available in the electronic medical record as of November 2025.				
[b] Values provided by the vendor that were not directly measured but calculated from other measured components.				
[c] Hedges' *g* for continuous variables (T2D+Obesity – controls) and odds ratios for categorical variables.				
* Indicates statistical significance ($p < 0.05$).				
T2D, Type 2 Diabetes; BMI, Body mass index; HbA1c, Hemoglobin A1c; HOMA-IR, Homeostatic Model Assessment of Insulin Resistance; HDL, High-density lipoprotein; LDL, Low-density lipoprotein; IL-6, Interleukin-6; MAP, Mean arterial pressure; FPG, Fasting plasma glucose; N/A, Not applicable.				

Metformin use was common in participants with T2D+Obesity (79%) and absent in controls. Statin-use was similar between the groups ($p > 0.05$), while anti-hypertensive medication use was greater in participants with T2D+Obesity ($p < 0.001$); however, the measured blood pressure did not differ significantly between the groups ($p > 0.05$).

Differences in CBF

Two control participants were excluded from the CBF analysis because of a blooming ASL signal observed in large arteries, potentially due to blood transit times longer than the post-label delay. Both excluded participants were from the control group. After age and sex adjustment, the CBF was observed to be greater in control participants (controls > T2D+Obesity) in three significant clusters at the applied statistical threshold ($p < 0.001$; extent threshold > = 10 contiguous voxels). No clusters resulted when the contrast was switched (T2D+Obesity > controls). The cluster characteristics are summarized in Table 2.

Table 2
Cluster and peak region characteristics where CBF was significantly lower in participants with T2D+Obesity compared with control participants. Region labels were obtained from the Automated Anatomical Labeling Atlas version 3 (AAL3).

Cluster	Size (voxels)	Cluster level $p_{FWE-corr}$	Peak T-score	MNI coordinates (x, y, z)	Hemisphere	Anatomical regions
1	1292	0.020	4.32	-8, -92, -4	Left	Calcarine fissure
			4.13	-10, -100, 4	Left	Superior occipital gyrus
			4.08	-20, -100, 0	Left	Middle occipital gyrus
			4.01	-36, -84, 2	Left	Middle occipital gyrus
			3.95	-18, -92, -4	Left	Middle occipital gyrus
			3.91	10, -98, 10	Right	Cuneus
			3.81	24, -96, 8	Right	Middle occipital gyrus
2	145	0.443	4.10	-34, -60, -22	Left	Lobule VI of the cerebellum
3	37	0.662	3.75	36, -84, 4	Right	Middle occipital gyrus

Briefly, the largest and most significant cluster (voxels = 1292; peak t-score = 4.32) was centered around the left calcarine fissure and surrounding primary visual cortex (PVC) [60], extending into the left superior and middle occipital gyri, as well as the right cuneus. This main cluster survived FWE-correction (p_{FWE} = 0.020). Significant clusters were also observed in the left cerebellar lobule VI (voxels = 145; peak t-score = 4.10) and the right middle occipital gyrus (voxels = 37; peak t-score = 3.75), but these did not survive FWE-correction. A voxel-wise CBF t-score map is shown in Fig. 1a, with corresponding sagittal, axial, and coronal views.

Figure 1b displays mean unadjusted CBF values for the combined cluster. The participants with T2D+Obesity exhibited a mean CBF of 36.4 ± 12.1 mL/100 g/min, approximately 37% lower than that of the controls (57.8 ± 15.6 mL/100 g/min).

Structural differences

Age- and sex-adjusted structural measures were examined from the same sample used in the CBF analysis (*N* = 30). Normalized cerebral cortical volume did not differ significantly between the groups (T2D+Obesity: 27.5% ± 1.82, Controls: 28.1% ± 1.23; *p* = 0.566), nor did the mean cortical thickness

(T2D+Obesity: 2.34 mm ± 0.0942, Controls: 2.38 mm ± 0.0714; $p = 0.323$). Normalized regional volumes and regional cortical thickness measures did not differ between the groups in any of the prespecified ROIs corresponding to the significant CBF clusters (all $p > 0.05$). Normalized WMH volume also did not differ between the groups (T2D+Obesity: 0.256% ± 0.245, Controls: 0.144% ± 0.083; $p = 0.183$). FreeSurfer-derived structural measures are reported in Supplementary Table 1.

Neuropsychological outcomes

Results of the neuropsychological assessment are shown in Table 3. Compared with the controls, the participants with T2D+Obesity had significantly lower scores on the RBANS List Learning ($p = 0.013$), Coding ($p = 0.040$), Attention ($p = 0.035$) and, the RBANS Global ($p = 0.022$) tests. The remaining RBANS subtest and domain scores did not differ significantly between the groups (all $p > 0.05$). The T2D+Obesity participants also had lower DKEFS CWIT switching trial performance, a measure of speed, inhibitory control, and mental set-shifting ($p = 0.001$). The Trail making test (TMT) parts A and B and the Texas card sorting test (TCST) logical sorts percentiles were not significantly different between the groups (all $p > 0.05$).

Table 3

Cognitive (neuropsychological) exam metrics are presented as percentile mean ± SD. RBANS and D-KEFS CWIT percentiles were derived from age-adjusted scaled scores (individual tests) or standard scores (domain composites) per standard testing procedure. TMT Part A (percentiles), and TMT Part B (percentiles), were derived from norm-referenced scores adjusted for age, sex, race, and education per standard testing procedure. TCST Logical Sorts (percentiles) was norm-referenced scores adjusted for age. Group differences were assessed using Mann–Whitney *U* tests. Effect sizes are reported as rank biserial correlation.

Repeatable Battery for the Assessment of Neuropsychological Status (RBANS)	**T2D+Obesity (*N* = 14)**	**Controls (*N* = 17[a])**	***p*-value**	**Effect size (Rank biserial)**
Individual Tests				
List learning	30.9 ± 28.7	63.0 ± 33.4	0.013*	-0.525
Story memory	47.5 ± 32.5	52.5 ± 30.3	0.620	-0.105
Semantic fluency[b]	34.6 ± 32.0	55.8 ± 35.4	0.066	-0.397
Digit span	46.6 ± 32.3	66.3 ± 25.1	0.076	-0.374
Coding	46.3 ± 31.8	69.2 ± 25.4	0.040*	-0.437
Figure copy	55.0 ± 26.3	63.5 ± 24.9	0.382	-0.185
Picture naming[b]	58.5 ± 19.3	56.4 ± 13.9	0.384	0.143
Story recall	50.5 ± 28.2	65.2 ± 28.8	0.136	-0.315
Figure recall	59.3 ± 28.1	67.1 ± 21.8	0.520	-0.139
Domain Composites				
Immediate memory	36.0 ± 26.0	57.1 ± 32.8	0.098	-0.353
Delayed memory	55.2 ± 26.0	63.7 ± 27.6	0.292	-0.227
Visuoconstruction/visuospatial	50.5 ± 27.7	65.2 ± 23.3	0.163	-0.298

Repeatable Battery for the Assessment of Neuropsychological Status (RBANS)	T2D+Obesity (*N* = 14)	Controls (*N* = 17[a])	*p*-value	Effect size (Rank biserial)
Language[b]	41.9 ± 24.7	59.3 ± 27.6	0.058	-0.411
Attention	46.4 ± 31.7	70.7 ± 21.0	0.035*	-0.450
Global	44.0 ± 27.9	66.3 ± 24.8	0.022*	-0.487
Delis–Kaplan Executive Function System Color and Word Interference Test (D-KEFS CWIT)[c]				
Color naming	47.7 ± 27.0	50.5 ± 27.4	0.757	-0.072
Word reading	51.6 ± 25.3	59.0 ± 18.6	0.488	-0.154
Interference	48.6 ± 31.4	69.3 ± 19.3	0.076	-0.389
Switching	41.3 ± 33.9	78.5 ± 20.4	0.001*	-0.712
Trail Making Test (TMT) – Part A	48.3 ± 33.8	60.0 ± 31.7	0.382	-0.189
Trail Making Test (TMT) – Part B	41.7 ± 31.0	60.1 ± 29.9	0.103	-0.349
Texas Card Sorting Test (TCST) – Logical Sorts[d]	49.4 ± 32.0	69.8 ± 28.4	0.172	-0.299

Repeatable Battery for the Assessment of Neuropsychological Status (RBANS)	T2D+Obesity (*N* = 14)	Controls (*N* = 17[a])	*p*-value	Effect size (Rank biserial)

[a] One participant was excluded from all neuropsychological analyses secondary to significant language-based barriers.

[b] One participant, for whom English was a second language, was excluded only from language-dependent measures.

[c] Two participants were unable to complete the D-KEFS CWIT secondary to color vision deficiency.

[d] One participant was unable to complete the TCST secondary to color vision deficiency.

* Indicates statistical significance ($p < 0.05$)

SD, Standard deviation

Supplementary Table

Associations between CBF, clinical, and neuropsychological tests

Across the entire sample, we observed that HbA1c, fasting plasma glucose, HOMA-IR, insulin, and leptin were each negatively associated with combined cluster CBF, after adjustment for age and sex (see Fig. 2 for selected associations). HDL was the only variable that was positively associated with combined cluster CBF ($p = 0.018$; Fig. 2c). The association between HDL and CBF remained significant after further adjustment for statin use in addition to age and sex (p = 0.024). Leptin was negatively associated with CBF (p = 0.019). The association between leptin and CBF was attenuated and no longer statistically significant after adjustment for BMI (p = 0.529) or waist-to-height ratio (p = 0.501), suggesting that the observed relationship was largely driven by adiposity. LDL, total cholesterol, and adiponectin levels were not significantly associated with CBF (all $p > 0.05$).

Association analyses were then performed between neuropsychological outcomes and residualized CBF values. Across all the participants, the age-residualized combined cluster CBF was positively correlated with the RBANS global percentile ($r = 0.500$, $p = 0.003$; Fig. 3a) and the RBANS list learning, a task that evaluates immediate verbal learning and recall ($r = 0.421$, $p = 0.013$; Fig. 3b). We also observed a positive correlation between the age-residualized combined cluster CBF and D-KEFS switching percentile ($r = 0.401$, $p = 0.022$; Fig. 3c)

Discussion

To our knowledge, this is the first T2D imaging study to integrate the 2014 ASL consensus recommendations with comprehensive neuropsychological, blood marker, and structural brain analyses. As a pilot study, we demonstrated that 1) older adults with T2D+Obesity exhibited both posterior hypoperfusion and poorer cognitive performance in list learning, attention, and executive function tasks in the absence of structural deficits. Across all participants, we observed 2) negative associations between combined cluster CBF and poor blood markers, i.e., higher HbA1c, HOMA-IR, FPG, insulin, and leptin are associated with lower CBF, and 3) positive associations between combined cluster CBF and cognitive performance. These results provide insights into the local and systemic mechanisms that may contribute to elevated risk of ADRD among older adults with T2D and obesity.

Interpretation of Clinical Markers and Neuropsychological Outcomes

The participants were well-matched for age, sex, education, and blood pressure. Participants with T2D were selected to have obesity (median BMI, 32.74 kg/m2 [IQR, 31.2–34.2]); therefore, the findings may not generalize to individuals with T2D who are overweight, lean, or have substantially different degrees of adiposity. As expected, markers of glycemia and insulin resistance were higher in participants with T2D+Obesity. On the basis of the mean HbA1c (6.7 ± 0.69%), our T2D+Obesity cohort may be characterized as having controlled T2D, according to the American Diabetes Association guidelines (HbA1c of < 7.0% in nonpregnant adults without significant risk of hypoglycemia) [61]. Although there are currently no clinical guidelines to define insulin resistance based on HOMA-IR values, one large U.S.-based study of metabolic syndrome proposed a cutoff of > 2.73 in the general adult population [62]. By this definition, the T2D+Obesity group (5.6 ± 2.9) was well above this threshold, whereas control participants (2.2 ± 1.8) fell slightly below this threshold. LDL and total cholesterol were significantly lower in the T2D+Obesity, which may be partially attributable to greater statin use among T2D+Obesity group (71% vs 44%), although statin use did not reach statistical significance between the groups. HDL was greater in control participants, and, interestingly, positively associated with combined cluster CBF. Because statin therapy may influence lipid profiles and vascular function, we performed a sensitivity analysis adjusting for statin use. The HDL association remained significant after adjustment, suggesting that the observed relationship is not solely attributable to statin exposure, although residual confounding cannot be entirely excluded. HDL is widely considered protective against cardiovascular events [63] and has been previously associated with increased cerebral perfusion in depression [64] and multiple sclerosis [65]. The T2D+Obesity group presented elevated blood leptin and reduced adiponectin, which is consistent with insulin resistance and adipose tissue dysfunction [66, 67]. Only leptin, however, was found to be negatively associated with combined cluster CBF. Although leptin was associated with CBF in the primary analysis, this relationship was no longer significant after adjustment for BMI or waist-to-height ratio. These findings suggest that adiposity may account for much of the observed association and highlight the close interrelationship between leptin and obesity-related metabolic dysfunction. The large between-group differences in HbA1c, HOMA-IR, and leptin reflect the intentional recruitment of

older adults with T2D and obesity and should be considered when interpreting the generalizability of the findings to populations with less severe metabolic impairment.

Antihypertensive medication use was not associated with significant differences in CBF after accounting for group status, and no significant within-group differences were observed. These findings suggest that antihypertensive medication use is unlikely to be a major contributor to the reduced CBF observed in the T2D+obesity group.

A key strength of this study was the incorporation of comprehensive neuropsychological testing. Across all neuropsychological outcomes where significant group differences were observed, participants with T2D+Obesity had lower scores (although all scores still fell within clinically normal ranges). Notably, these differences were not restricted to one domain of cognition but observed across several domains (list learning, coding, attention, and aspects of executive function). The deficit in list learning may also reflect an attention-driven encoding difficulty rather than a primary memory storage problem, given that other immediate memory and delayed memory scores did not differ between groups. These findings overlap with patterns associated with cerebrovascular-related cognitive difficulties, including vascular cognitive impairment and dementia (VCID) [68].

There is a large body of evidence linking T2D to poorer cognitive performance and increased dementia risk [69]. In contrast, the relationship between obesity and cognition in older adults is more complex, with prior studies reporting positive, negative, or no associations between BMI and cognitive performance [18–21]. Moreover, the contribution of obesity to cognitive outcomes in individuals with T2D remains incompletely understood. In the present study, participants with T2D and obesity exhibited significant central adiposity, reflected by an elevated waist-to-height ratio, a measure previously associated with poorer cognitive function in older adults (N = 1709) [70]. Our findings extend this literature by examining brain physiology in older adults with both T2D and obesity, a population at particularly high risk for cerebrovascular dysfunction and cognitive decline.

Consolidation of imaging results with cognitive function outcomes

We observed the most prominent hypoperfusion in the occipital lobe, centered at the PVC and extending into the superior occipital gyrus. Beyond visual processing, these regions contribute to visual and visuospatial attention, functions that are often impaired in early ADRD [71–74]. Consistent with these findings, participants with T2D and obesity demonstrated poorer executive function, particularly cognitive flexibility (CWIT), which was associated with reduced CBF. Notably, similar tasks for example, the Stroop paradigm recruit visual attention networks, and impairments in Stroop performance and CWIT have been reported in individuals at elevated risk for AD and in patients with early VCID [75–78]. Taken together, these findings suggest that occipital hypoperfusion may reflect dysfunction within visual attention networks and represent an early cerebrovascular process associated with cognitive decline and ADRD risk.

T2D is associated with endothelial dysfunction and microvascular damage [79], and the occipital lobe may be particularly vulnerable to these changes. Prior ASL studies have similarly reported occipital hypoperfusion in T2D, including reduced perfusion and prolonged bolus arrival time in the middle occipital gyrus [38, 43]. The high metabolic demand of the occipital lobe, together with potentially less robust autoregulation in the posterior circulation, may increase susceptibility to vascular dysfunction in this region [80, 81].

We also noted some hypoperfusion in the left cerebellum. To our knowledge, this has been reported only once previously in patients with T2D using ASL methods [82]. Although the cerebellum is not classically emphasized in traditional ADRD models, it plays an established role in cognitive function and mood. Consensus papers have noted the role of the cerebellum, particularly posterior lateral cerebellar areas (e.g., the 6th lobule), in higher-order cognition, such as encoding and language processing [83, 84]. This finding should be interpreted cautiously, however, as this cluster did not survive multiple-comparisons corrections and accounted for only a small portion of the overall spatial pattern observed in our results.

Despite appropriate glycemic control in our participants with T2D+Obesity, prominent regional hypoperfusion was still observed, and lower CBF was strongly associated with diabetic markers of disease. This persistence suggests that cerebrovascular damage associated with T2D may not be fully reversible through conventional metabolic management alone, suggesting an additional vascular contribution. Additionally, we observed that CBF was positively associated with global cognition. These associations were observed even in the absence of key structural changes such as cortical thickness, volume, or WMH differences. Prior literature has identified CBF alterations during the preclinical and early symptomatic stages of AD, and some longitudinal evidence suggests that reduced regional perfusion precedes substantial structural brain changes [91–95], and CBF alterations are associated with cognitive decline in VCID [79]. Accordingly, the CBF changes observed here may reflect early imaging changes occurring prior to clinically significant cognitive impairment. However, these findings should be interpreted cautiously given the pilot nature of the study and require confirmation in larger, independent, and longitudinal cohorts.

Limitations, future steps, and conclusions

This study has several limitations. First, the sample size was modest and limited to a single center, which may limit generalizability. Second, differences in medication use between groups may have influenced both metabolic and cerebrovascular measures and represent a potential source of residual confounding, which cannot be disentangled. Third, only CBF in the bilateral occipital cluster survived cluster-level FWE correction. The remaining voxel-wise cluster in the cerebellum did not survive FWE correction, and the neuropsychological, and association analyses were also not corrected for multiple comparisons and should therefore be interpreted cautiously. Fourth, the findings from this study may not generalize to individuals with T2D who are overweight, lean, or have substantially different degrees of adiposity. Fifth, we did not apply partial volume correction to the CBF analyses, instead we evaluated structural measures separately to reduce model complexity and the risk of overfitting. Sixth, CBF was measured using a single-delay ASL acquisition. Although this approach is widely used and provides

robust estimates of perfusion, it does not permit separate quantification of arterial transit time, which may itself be altered in T2D and obesity. Future studies incorporating multi-delay ASL could provide additional insight into the relative contributions of delayed arterial arrival and reduced tissue perfusion. Seventh, AD-specific biomarkers, such as amyloid-β and tau measures, were not acquired. Consequently, the relationship between the observed cerebrovascular abnormalities and underlying AD pathology could not be directly assessed. Eighth, peripheral vascular and endothelial function were not assessed, limiting our ability to determine whether systemic vascular dysfunction contributed to the observed cerebral perfusion changes. Finally, the cross-sectional design precludes conclusions regarding causality or temporal sequencing. Longitudinal studies are needed to determine whether the observed cerebrovascular alterations precede cognitive decline and contribute to future ADRD risk.

Future work should examine whether targeted treatment of obesity and metabolic dysfunction in individuals with T2D, particularly with GLP-1 receptor agonists or related therapies, can favorably modify regional cerebral and cerebellar perfusion. Since dementia often reflects mixed pathology, the incorporation of biomarkers of AD-related pathology (i.e., β-amyloid and phosphorylated tau) and VCID-related pathology (i.e., subcortical infarcts on diffusion weighted imaging) may further clarify the mechanistic links between vascular and metabolic disease and ADRD expression. Methodological extensions could include multi-delay pCASL, as well as multimodal MRI techniques to investigate functional connectivity and microvascular integrity, including blood-brain barrier dysfunction. Longitudinal designs will be essential to determine whether the observed perfusion changes precede or track cognitive decline.

In conclusion, we report that posterior hypoperfusion in older adults with T2D and obesity is associated with subtle but measurable cognitive changes, even in the absence of overt structural brain changes. Further research is needed to outline the vascular and metabolic mechanisms by which T2D and obesity influence ADRD risk. Successful translation of this area of research in larger groups may lead to improved risk prediction and novel interventions that reduce the burden of ADRD and improve the quality of life for millions of patients.

Declarations

Author Contribution Statement

Binu Thomas: Conceptualization, methodology, validation, formal analysis, investigation, resources, data curation, writing – review & editing, supervision, project administration, funding acquisition

Mohamad N. Elsharydah: Software, formal analysis, data curation, writing – original draft, visualization

Jeff Schaffert: Validation, formal analysis, investigation, resources, data curation, writing – review & editing, supervision

Anujit Saha: Data curation, investigation, writing – review & editing

Jack Kaufman: Investigation, data curation

Jennine Leary: Investigation, resources, data curation

Alison Jin: Investigation, resources

Jaime P. Almandoz: Investigation, writing – review & editing, supervision

Ethics Approval and Consent To Participate

The study was conducted in accordance with the Declaration of Helsinki. It received approval by the Institutional Review Board (IRB) at UT Southwestern Medical Center (IRB approval number: STU-2023-0388). All participants provided written informed consent prior to participation.

Consent for Publication

Not applicable.

Disclosures

Dr. Jaime Almandoz is a Consultant at AbbVie, Amgen, Boehringer Ingelheim, Eli Lilly, Haleon, Kailera, Metsera/Pfizer, Novo Nordisk, Rivus, Rhythm Pharmaceuticals, and Wave Life Sciences. The other authors declare no competing interests.

Funding

was provided by the NIH grant P30 DK127984 and the Cancer Prevention and Research Institute of Texas (CPRIT) grant RR180056. The funding sources were not involved in the study design, collection, analysis or interpretation of the data; writing of the report; or the decision to submit the article for publication.

Author Contribution

Mohamad N. Elsharydah: Software, formal analysis, data curation, writing – original draft, visualizationJeff Schaffert: Validation, formal analysis, investigation, resources, data curation, writing – review & editing, supervisionAnujit Saha: Data curation, investigation, writing – review & editingJack Kaufman: Investigation, data curationJennine Leary: Investigation, resources, data curationAlison Jin: Investigation, resourcesJaime P. Almandoz: Investigation, writing – review & editing, supervisionBinu P.

Thomas: Conceptualization, methodology, validation, formal analysis, investigation, resources, data curation, writing – review & editing, supervision, project administration, funding acquisition

Acknowledgement

The ASL perfusion software used in this study was provided by the Stevens Neuroimaging and Informatics Institute at the University of Southern California. Portions of the licensed technology were developed by The Regents of the University of California, on behalf of its Los Angeles campus.

Data Availability

The datasets used in this study are available from the corresponding author upon reasonable request. Please allow reasonable time for response. All the results analyzed supporting the findings of this study are presented within the article.

References

1. Nanda, M., Sharma, R., Mubarik, S., Aashima, A. & Zhang, K. Type-2 Diabetes Mellitus (T2DM): Spatial-temporal Patterns of Incidence, Mortality and Attributable Risk Factors from 1990 to 2019 among 21 World Regions. *Endocrine* **77** (3), 444–454. 10.1007/s12020-022-03125-5 (2022).
2. Collaborators, G. B. D. D. Global, regional, and national burden of diabetes from 1990 to 2021, with projections of prevalence to 2050: a systematic analysis for the Global Burden of Disease Study 2021. *Lancet* **402** (10397), 203–234. 10.1016/S0140-6736(23)01301-6 (2023).
3. Stolar, M. Glycemic control and complications in type 2 diabetes mellitus. *Am. J. Med.* **123** (3 Suppl), S3–11. 10.1016/j.amjmed.2009.12.004 (2010).
4. Livingston, G. et al. Dementia prevention, intervention, and care: 2024 report of the Lancet standing Commission. *Lancet* **404** (10452), 572–628. 10.1016/S0140-6736(24)01296-0 (2024).
5. Athanasaki, A. et al. Type 2 Diabetes Mellitus as a Risk Factor for Alzheimer's Disease: Review and Meta-Analysis. *Biomedicines* **10** (4). 10.3390/biomedicines10040778 (2022).
6. Roberts, R. O. et al. Association of diabetes with amnestic and nonamnestic mild cognitive impairment. *Alzheimers Dement.* **10** (1), 18–26. 10.1016/j.jalz.2013.01.001 (2014).
7. Seo, D. H. et al. Association between Age at Diagnosis of Type 2 Diabetes and Subsequent Risk of Dementia and Its Major Subtypes. *J. Clin. Med.* **13** (15). 10.3390/jcm13154386 (2024).
8. Kellar, D. & Craft, S. Brain insulin resistance in Alzheimer's disease and related disorders: mechanisms and therapeutic approaches. *Lancet Neurol.* **19** (9), 758–766. 10.1016/S1474-4422(20)30231-3 (2020).
9. Biessels, G. J. & Despa, F. Cognitive decline and dementia in diabetes mellitus: mechanisms and clinical implications. *Nat. Rev. Endocrinol.* **14** (10), 591–604. 10.1038/s41574-018-0048-7 (2018).

10. Arnold, S. E. et al. Brain insulin resistance in type 2 diabetes and Alzheimer disease: concepts and conundrums. *Nat. Rev. Neurol.* **14** (3), 168–181. 10.1038/nrneurol.2017.185 (2018).
11. Shome, G. et al. Bridging Pancreatic Amyloidosis and Neurodegeneration: The Emerging Role of Amylin in Diabetic Dementia. *Int. J. Mol. Sci.* **26** (11). 10.3390/ijms26115021 (2025).
12. Sims-Robinson, C., Kim, B., Rosko, A. & Feldman, E. L. How does diabetes accelerate Alzheimer disease pathology? *Nat. Rev. Neurol.* **6** (10), 551–559. 10.1038/nrneurol.2010.130 (2010).
13. Ruze, R. et al. Obesity and type 2 diabetes mellitus: connections in epidemiology, pathogenesis, and treatments. *Front. Endocrinol. (Lausanne)*. **14**, 1161521. 10.3389/fendo.2023.1161521 (2023).
14. Albanese, E. et al. Body mass index in midlife and dementia: Systematic review and meta-regression analysis of 589,649 men and women followed in longitudinal studies. *Alzheimers Dement. (Amst)*. **8**, 165–178. 10.1016/j.dadm.2017.05.007 (2017).
15. Natale, G., Zhang, Y., Hanes, D. W. & Clouston, S. A. Obesity in Late-Life as a Protective Factor Against Dementia and Dementia-Related Mortality. *Am. J. Alzheimers Dis. Other Demen*. **38**, 15333175221111658. 10.1177/15333175221111658 (2023).
16. Xing, Z., Long, C., Hu, X. & Chai, X. Obesity is associated with greater cognitive function in patients with type 2 diabetes mellitus. *Front. Endocrinol. (Lausanne)*. **13**, 953826. 10.3389/fendo.2022.953826 (2022).
17. Mansur, R. B. et al. Determinants of cognitive function in individuals with type 2 diabetes mellitus: A meta-analysis. *Ann. Clin. Psychiatry*. **30** (1), 38–50 (2018).
18. Ge, J., Han, Y., Peng, S., Zhang, S. & Zheng, L. U-shaped association between BMI and cognitive impairment in middle-aged and older adults with type 2 diabetes: effect modification by lifestyle and exercise. *Front. Public. Health*. **13**, 1675383. 10.3389/fpubh.2025.1675383 (2025).
19. Drake, J. A. et al. Multilevel and multidimensional features of socioeconomic status and cognitive function in older adulthood: a cross-sectional analysis of the IGNITE study. *Lancet Reg. Health Am.* **50**, 101206. 10.1016/j.lana.2025.101206 (2025).
20. Morys, F., Dadar, M. & Dagher, A. Association Between Midlife Obesity and Its Metabolic Consequences, Cerebrovascular Disease, and Cognitive Decline. *J. Clin. Endocrinol. Metab.* **106** (10), e4260–e74. 10.1210/clinem/dgab135 (2021).
21. Li, F. et al. Frailty and its combined effects with lifestyle factors on cognitive function: a cross-sectional study. *BMC Geriatr.* **23** (1), 79. 10.1186/s12877-023-03761-0 (2023).
22. O'Brien, P. D., Hinder, L. M., Callaghan, B. C. & Feldman, E. L. Neurological consequences of obesity. *Lancet Neurol.* **16** (6), 465–477. 10.1016/S1474-4422(17)30084-4 (2017).
23. Moh, M. C. et al. Association of traditional and novel measures of central obesity with cognitive performance in older multi-ethnic Asians with type 2 diabetes. *Clin. Obes.* **10** (2), e12352. 10.1111/cob.12352 (2020).
24. Anwar, N. et al. Cognition and brain oxygen metabolism improves after bariatric surgery-induced weight loss: A pilot study. *Front. Endocrinol. (Lausanne)*. **13**, 954127. 10.3389/fendo.2022.954127 (2022).

25. Tucker, W. J. et al. Impact of bariatric surgery on cerebral vascular reactivity and cognitive function: a non-randomized pilot study. *Pilot Feasibility Stud.* **6**, 21. 10.1186/s40814-020-00569-2 (2020).
26. Iutaka, T. et al. Arterial Spin Labeling: Techniques, Clinical Applications, and Interpretation. *Radiographics* **43** (1), e220088. 10.1148/rg.220088 (2023).
27. Ho, M. L. Arterial spin labeling: Clinical applications. *J. Neuroradiol.* **45** (5), 276–289. 10.1016/j.neurad.2018.06.003 (2018).
28. Romano, A. et al. Does arterial spin labelling represent a valid alternative to other MR perfusion techniques in neuro-oncology? *Radiol. Med.* **130** (9), 1489–1502. 10.1007/s11547-025-02048-1 (2025).
29. Thomas, B. P., Liu, P., Park, D. C., van Osch, M. J. & Lu, H. Cerebrovascular reactivity in the brain white matter: magnitude, temporal characteristics, and age effects. *J. Cereb. Blood Flow. Metab.* **34** (2), 242–247. 10.1038/jcbfm.2013.194 (2014).
30. Ferreira, R. & Bastos-Leite, A. J. Arterial spin labelling magnetic resonance imaging and perfusion patterns in neurocognitive and other mental disorders: a systematic review. *Neuroradiology* **66** (7), 1065–1081. 10.1007/s00234-024-03323-0 (2024).
31. Alsop, D. C. et al. Recommended implementation of arterial spin-labeled perfusion MRI for clinical applications: A consensus of the ISMRM perfusion study group and the European consortium for ASL in dementia. *Magn. Reson. Med.* **73** (1), 102–116. 10.1002/mrm.25197 (2015).
32. Russo, A. et al. Arterial spin labeling MRI applied to migraine: current insights and future perspectives. *J. Headache Pain*. **24** (1), 71. 10.1186/s10194-023-01597-y (2023).
33. Thomas, B. P. et al. Hippocampal and rostral anterior cingulate blood flow is associated with affective symptoms in chronic traumatic brain injury. *Brain Res.* **1771**, 147631. 10.1016/j.brainres.2021.147631 (2021).
34. Thomas, B. P. et al. Brain Perfusion Change in Patients with Mild Cognitive Impairment After 12 Months of Aerobic Exercise Training. *J. Alzheimers Dis.* **75** (2), 617–631. 10.3233/JAD-190977 (2020).
35. Feron, J. et al. Cerebral blood flow and arterial transit time responses to exercise training in older adults. *Neuroimage* **303**, 120919. 10.1016/j.neuroimage.2024.120919 (2024).
36. Thomas, B. P. et al. Life-long aerobic exercise preserved baseline cerebral blood flow but reduced vascular reactivity to CO2. *J. Magn. Reson. Imaging*. **38** (5), 1177–1183. 10.1002/jmri.24090 (2013).
37. De Vis, J. B. et al. Arterial-spin-labeling (ASL) perfusion MRI predicts cognitive function in elderly individuals: A 4-year longitudinal study. *J. Magn. Reson. Imaging*. **48** (2), 449–458. 10.1002/jmri.25938 (2018).
38. Liu, J. et al. Cerebral Blood Flow Alterations in Type 2 Diabetes Mellitus: A Systematic Review and Meta-Analysis of Arterial Spin Labeling Studies. *Front. Aging Neurosci.* **14**, 847218. 10.3389/fnagi.2022.847218 (2022).
39. Zhong, Y. L., Hu, R. Y. & Huang, X. Aberrant Neurovascular Coupling in Diabetic Retinopathy Using Arterial Spin Labeling (ASL) and Functional Magnetic Resonance Imaging (fMRI) methods. *Diabetes*

Metab. Syndr. Obes. **17**, 2809–2822. 10.2147/DMSO.S465103 (2024).

40. Huang, X., Wen, Z., Tong, Y., Qi, C. X. & Shen, Y. Altered resting cerebral blood flow specific to patients with diabetic retinopathy revealed by arterial spin labeling perfusion magnetic resonance imaging. *Acta Radiol.* **62** (4), 524–532. 10.1177/0284185120932391 (2021).
41. Cui, Y. et al. Cerebral perfusion alterations in type 2 diabetes and its relation to insulin resistance and cognitive dysfunction. *Brain Imaging Behav.* **11** (5), 1248–1257. 10.1007/s11682-016-9583-9 (2017).
42. Zhang, D. et al. Neuroimaging endophenotypes of type 2 diabetes mellitus: a discordant sibling pair study. *Quant. Imaging Med. Surg.* **9** (6), 1000–1013. 10.21037/qims.2019.05.18 (2019).
43. Shen, Y. et al. Cerebral Hemodynamic and White Matter Changes of Type 2 Diabetes Revealed by Multi-TI Arterial Spin Labeling and Double Inversion Recovery Sequence. *Front. Neurol.* **8**, 717. 10.3389/fneur.2017.00717 (2017).
44. Chau, A. C. M. et al. Impaired cerebral blood flow in type 2 diabetes mellitus - A comparative study with subjective cognitive decline, vascular dementia and Alzheimer's disease subjects. *Neuroimage Clin.* **27**, 102302. 10.1016/j.nicl.2020.102302 (2020).
45. Jansen, J. F. et al. Cerebral blood flow, blood supply, and cognition in Type 2 Diabetes Mellitus. *Sci. Rep.* **6** (1), 10. 10.1038/s41598-016-0003-6 (2016).
46. Xiao, Y., Hong, X., Neelagar, R. & Mo, H. Association between glycated hemoglobin A1c levels, control status, and cognitive function in type 2 diabetes: a prospective cohort study. *Sci. Rep.* **15** (1), 5011. 10.1038/s41598-025-89374-6 (2025).
47. Moran, C. et al. Glycemic Control Over Multiple Decades and Dementia Risk in People With Type 2 Diabetes. *JAMA Neurol.* **80** (6), 597–604. 10.1001/jamaneurol.2023.0697 (2023).
48. Bangen, K. J. et al. Reduced Regional Cerebral Blood Flow Relates to Poorer Cognition in Older Adults With Type 2 Diabetes. *Front. Aging Neurosci.* **10**, 270. 10.3389/fnagi.2018.00270 (2018).
49. Oh, D. J. et al. Brain Structural Alterations, Diabetes Biomarkers, and Cognitive Performance in Older Adults With Dysglycemia. *Front. Neurol.* **12**, 766216. 10.3389/fneur.2021.766216 (2021).
50. Matthews, D. R. et al. Homeostasis model assessment: insulin resistance and beta-cell function from fasting plasma glucose and insulin concentrations in man. *Diabetologia* **28** (7), 412–419. 10.1007/BF00280883 (1985).
51. Kilroy, E. et al. Reliability of two-dimensional and three-dimensional pseudo-continuous arterial spin labeling perfusion MRI in elderly populations: comparison with 15O-water positron emission tomography. *J. Magn. Reson. Imaging*. **39** (4), 931–939. 10.1002/jmri.24246 (2014).
52. Li, Y. et al. ASL-MRICloud: An online tool for the processing of ASL MRI data. *NMR Biomed.* **32** (2), e4051. 10.1002/nbm.4051 (2019).
53. Gaser, C., Dahnke, R., Thompson, P. M., Kurth, F. & Luders, E. The Alzheimer's Disease Neuroimaging I. CAT: a computational anatomy toolbox for the analysis of structural MRI data. *Gigascience* **13** 10.1093/gigascience/giae049 (2024).

54. Randolph, C., Tierney, M. C., Mohr, E. & Chase, T. N. The Repeatable Battery for the Assessment of Neuropsychological Status (RBANS): preliminary clinical validity. *J. Clin. Exp. Neuropsychol.* **20** (3), 310–319. 10.1076/jcen.20.3.310.823 (1998).
55. Armitage, S. G. Trail Making Test. (1946).
56. Lacritz, L. H., Kaser, A. N., Argueta-Ortiz, F., Hynan, L. S. & Cullum, C. M. Texas Card Sorting Test: a Brief Test of Executive Functioning with Age-Adjusted Norms and External Validation. *Arch. Clin. Neuropsychol.* **41** (2). 10.1093/arclin/acag004 (2026).
57. Delis, D. C., Kaplan, E. & Kramer, J. H. *Delis-Kaplan Executive Function System (D–KEFS)* (Psychological Corp, 2001).
58. Rolls, E. T., Huang, C. C., Lin, C. P., Feng, J. & Joliot, M. Automated anatomical labelling atlas 3. *Neuroimage* **206**, 116189. 10.1016/j.neuroimage.2019.116189 (2020).
59. Heaton, R. K. M. S., Taylor, M. J. & Grant, I. *Revised comprehensive norms for an expanded Halstead-Reitan Battery: demographically adjusted neuropsychological norms for African American and Caucasian adults* (Psychological Assessment Resources, 2004).
60. Grill-Spector, K. & Malach, R. The human visual cortex. *Annu. Rev. Neurosci.* **27**, 649–677. 10.1146/annurev.neuro.27.070203.144220 (2004).
61. American Diabetes Association Professional Practice Committee for D. 6. Glycemic Goals, Hypoglycemia, and Hyperglycemic Crises: Standards of Care in Diabetes-2026. Diabetes Care. ;49(Supplement_1):S132–S49. (2026). 10.2337/dc26-S006
62. Sumner, A. E. & Cowie, C. C. Ethnic differences in the ability of triglyceride levels to identify insulin resistance. *Atherosclerosis* **196** (2), 696–703. 10.1016/j.atherosclerosis.2006.12.018 (2008).
63. Nagao, M., Nakajima, H., Toh, R., Hirata, K. I. & Ishida, T. Cardioprotective Effects of High-Density Lipoprotein Beyond its Anti-Atherogenic Action. *J. Atheroscler Thromb.* **25** (10), 985–993. 10.5551/jat.RV17025 (2018).
64. Kang, L. et al. Dysregulated cerebral blood flow, rather than gray matter Volume, exhibits stronger correlations with blood inflammatory and lipid markers in depression. *Neuroimage Clin.* **41**, 103581. 10.1016/j.nicl.2024.103581 (2024).
65. Jakimovski, D. et al. High density lipoprotein cholesterol and apolipoprotein A-I are associated with greater cerebral perfusion in multiple sclerosis. *J. Neurol. Sci.* **418**, 117120. 10.1016/j.jns.2020.117120 (2020).
66. Ramakrishnan, N., Auger, K., Rahimi, N., Jialal, I. & Biochemistry Adiponectin. StatPearls. Treasure Island (FL)2025.
67. Zhao, Y. & Li, H. Association of serum leptin and insulin levels among type 2 diabetes mellitus patients: A case-control study. *Med. (Baltim).* **101** (41), e31006. 10.1097/MD.0000000000031006 (2022).
68. Cavanagh, L. & Paulsen, J. S. Neuropsychology and Vascular Cognitive Impairment and Dementia. *Neurol. Clin.* **42** (4), 809–820. 10.1016/j.ncl.2024.05.006 (2024).

69. Monette, M. C., Baird, A. & Jackson, D. L. A meta-analysis of cognitive functioning in nondemented adults with type 2 diabetes mellitus. *Can. J. Diabetes*. **38** (6), 401–408. 10.1016/j.jcjd.2014.01.014 (2014).
70. Tang, H., Li, Q. & Du, C. The association between waist-to-height ratio and cognitive function in older adults. *Nutr. Neurosci.* **27** (12), 1405–1412. 10.1080/1028415X.2024.2339729 (2024).
71. Somers, D. C., Dale, A. M., Seiffert, A. E. & Tootell, R. B. Functional MRI reveals spatially specific attentional modulation in human primary visual cortex. *Proc. Natl. Acad. Sci. U S A*. **96** (4), 1663–1668. 10.1073/pnas.96.4.1663 (1999).
72. Ress, D., Backus, B. T. & Heeger, D. J. Activity in primary visual cortex predicts performance in a visual detection task. *Nat. Neurosci.* **3** (9), 940–945. 10.1038/78856 (2000).
73. Rizzo, M., Anderson, S. W., Dawson, J., Myers, R. & Ball, K. Visual attention impairments in Alzheimer's disease. *Neurology* **54** (10), 1954–1959. 10.1212/wnl.54.10.1954 (2000).
74. Rosler, A. et al. Visual search in patients with subcortical vascular dementia: short fixations but long reaction times. *Dement. Geriatr. Cogn. Disord*. **20** (6), 375–380. 10.1159/000089104 (2005).
75. Chen, Q., Marshall, J. C., Weidner, R. & Fink, G. R. Zooming in and zooming out of the attentional focus: an FMRI study. *Cereb. Cortex*. **19** (4), 805–819. 10.1093/cercor/bhn128 (2009).
76. Harrison, B. J. et al. Functional connectivity during Stroop task performance. *Neuroimage* **24** (1), 181–191. 10.1016/j.neuroimage.2004.08.033 (2005).
77. Harrington, M. G. et al. Executive function changes before memory in preclinical Alzheimer's pathology: a prospective, cross-sectional, case control study. *PLoS One*. **8** (11), e79378. 10.1371/journal.pone.0079378 (2013).
78. Pantsiou, K. et al. Inhibitory Control, Task/Rule Switching, and Cognitive Planning in Vascular Dementia: Are There Any Differences From Vascular Aging? *Front. Aging Neurosci.* **10**, 330. 10.3389/fnagi.2018.00330 (2018).
79. van Sloten, T. T., Sedaghat, S., Carnethon, M. R., Launer, L. J. & Stehouwer, C. D. A. Cerebral microvascular complications of type 2 diabetes: stroke, cognitive dysfunction, and depression. *Lancet Diabetes Endocrinol.* **8** (4), 325–336. 10.1016/S2213-8587(19)30405-X (2020).
80. Ishii, K. et al. Regional difference in cerebral blood flow and oxidative metabolism in human cortex. *J. Nucl. Med.* **37** (7), 1086–1088 (1996).
81. Srichawla, B. S. & Garcia-Dominguez, M. A. Regional dynamic cerebral autoregulation across anterior and posterior circulatory territories: A detailed exploration and its clinical implications. *World J. Crit. Care Med.* **13** (4), 97149. 10.5492/wjccm.v13.i4.97149 (2024).
82. Dai, W. et al. The resting perfusion pattern associates with functional decline in type 2 diabetes. *Neurobiol. Aging*. **60**, 192–202. 10.1016/j.neurobiolaging.2017.09.004 (2017).
83. Koziol, L. F. et al. Consensus paper: the cerebellum's role in movement and cognition. *Cerebellum* **13** (1), 151–177. 10.1007/s12311-013-0511-x (2014).

84. Marien, P. et al. Consensus paper: Language and the cerebellum: an ongoing enigma. *Cerebellum* **13** (3), 386–410. 10.1007/s12311-013-0540-5 (2014).
85. Guo, C. C. et al. Network-selective vulnerability of the human cerebellum to Alzheimer's disease and frontotemporal dementia. *Brain* **139** (Pt 5), 1527–1538. 10.1093/brain/aww003 (2016).
86. Jacobs, H. I. L. et al. The cerebellum in Alzheimer's disease: evaluating its role in cognitive decline. *Brain* **141** (1), 37–47. 10.1093/brain/awx194 (2018).
87. Schaefer, A. et al. Early small vessel disease affects frontoparietal and cerebellar hubs in close correlation with clinical symptoms–a resting-state fMRI study. *J. Cereb. Blood Flow. Metab.* **34** (7), 1091–1095. 10.1038/jcbfm.2014.70 (2014).
88. Gellersen, H. M., Guell, X. & Sami, S. Differential vulnerability of the cerebellum in healthy ageing and Alzheimer's disease. *Neuroimage Clin.* **30**, 102605. 10.1016/j.nicl.2021.102605 (2021).
89. Samstag, C. L. et al. Neuropathological correlates of vulnerability and resilience in the cerebellum in Alzheimer's disease. *Alzheimers Dement.* **21** (2), e14428. 10.1002/alz.14428 (2025).
90. Acharya, A., Ren, P., Yi, L., Tian, W. & Liang, X. Structural atrophy and functional dysconnectivity patterns in the cerebellum relate to cerebral networks in svMCI. *Front. Neurosci.* **16**, 1006231. 10.3389/fnins.2022.1006231 (2022).
91. Bernetti, C. et al. Arterial Spin Labeling MRI in Alzheimer's Disease: A Systematic Review of Cerebral Perfusion Biomarkers. *J. Neuroimaging*. **35** (2), e70035. 10.1111/jon.70035 (2025).
92. Alsop, D. C., Dai, W., Grossman, M. & Detre, J. A. Arterial spin labeling blood flow MRI: its role in the early characterization of Alzheimer's disease. *J. Alzheimers Dis.* **20** (3), 871–880. 10.3233/JAD-2010-091699 (2010).
93. Wierenga, C. E., Hays, C. C. & Zlatar, Z. Z. Cerebral blood flow measured by arterial spin labeling MRI as a preclinical marker of Alzheimer's disease. *J. Alzheimers Dis.* **42** (Suppl 4), S411–S419. 10.3233/JAD-141467 (2014).
94. Binnewijzend, M. A. et al. Cerebral perfusion in the predementia stages of Alzheimer's disease. *Eur. Radiol.* **26** (2), 506–514. 10.1007/s00330-015-3834-9 (2016).
95. Mattsson, N. et al. Association of brain amyloid-beta with cerebral perfusion and structure in Alzheimer's disease and mild cognitive impairment. *Brain* **137** (Pt 5), 1550–1561. 10.1093/brain/awu043 (2014).

Figures

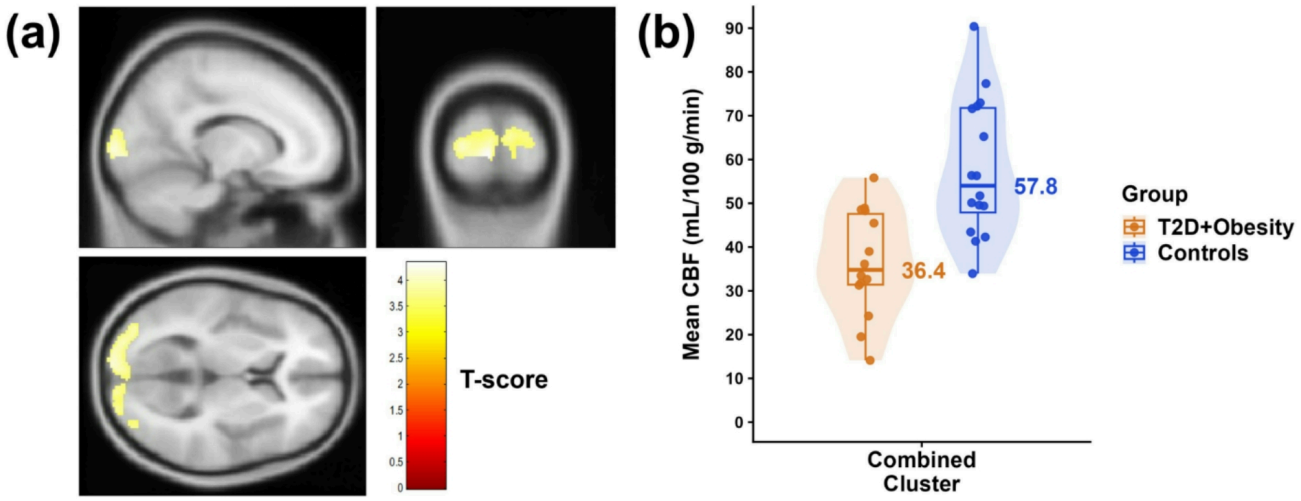


Figure 1

(a) Voxel-wise cerebral blood flow (CBF) comparison (T-score map) between control participants and participants with T2D+Obesity, displayed at the uncorrected voxel-wise threshold of $p < 0.001$ with a cluster extent threshold of 10 voxels, after adjustment for age and sex. Colored voxels represent clusters where CBF was lower in the T2D+Obesity group compared with the control group. Clusters are superimposed on an average T1 weighted image. Images are shown in neurological convention. The color bar represents T-score values. **(b)** Combined cluster means (unadjusted for age and sex) plotted for visualization. T2D, Type 2 Diabetes.

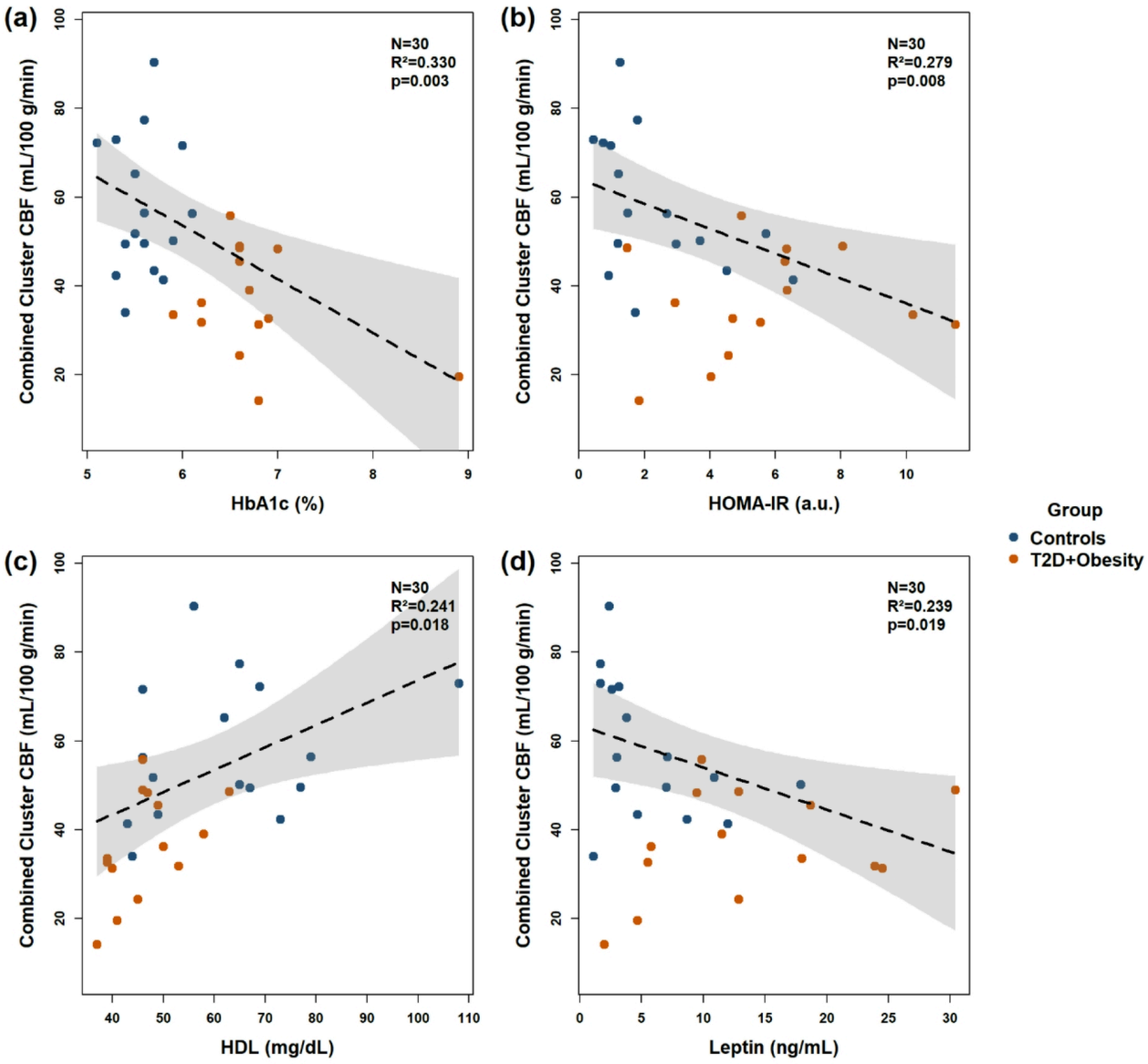


Figure 2

Selected associations between clinical markers and combined cluster CBF across all participants. Combined cluster CBF was inversely associated with **(a)** HbA1c (p = 0.003) and **(b)** HOMA-IR (p = 0.008), positively associated with **(c)** HDL (p = 0.018) and negatively associated with (d) Leptin (p = 0.019). All models were adjusted for age and sex. Gray color shaded bands represent 95% confidence intervals around the fitted regression line.

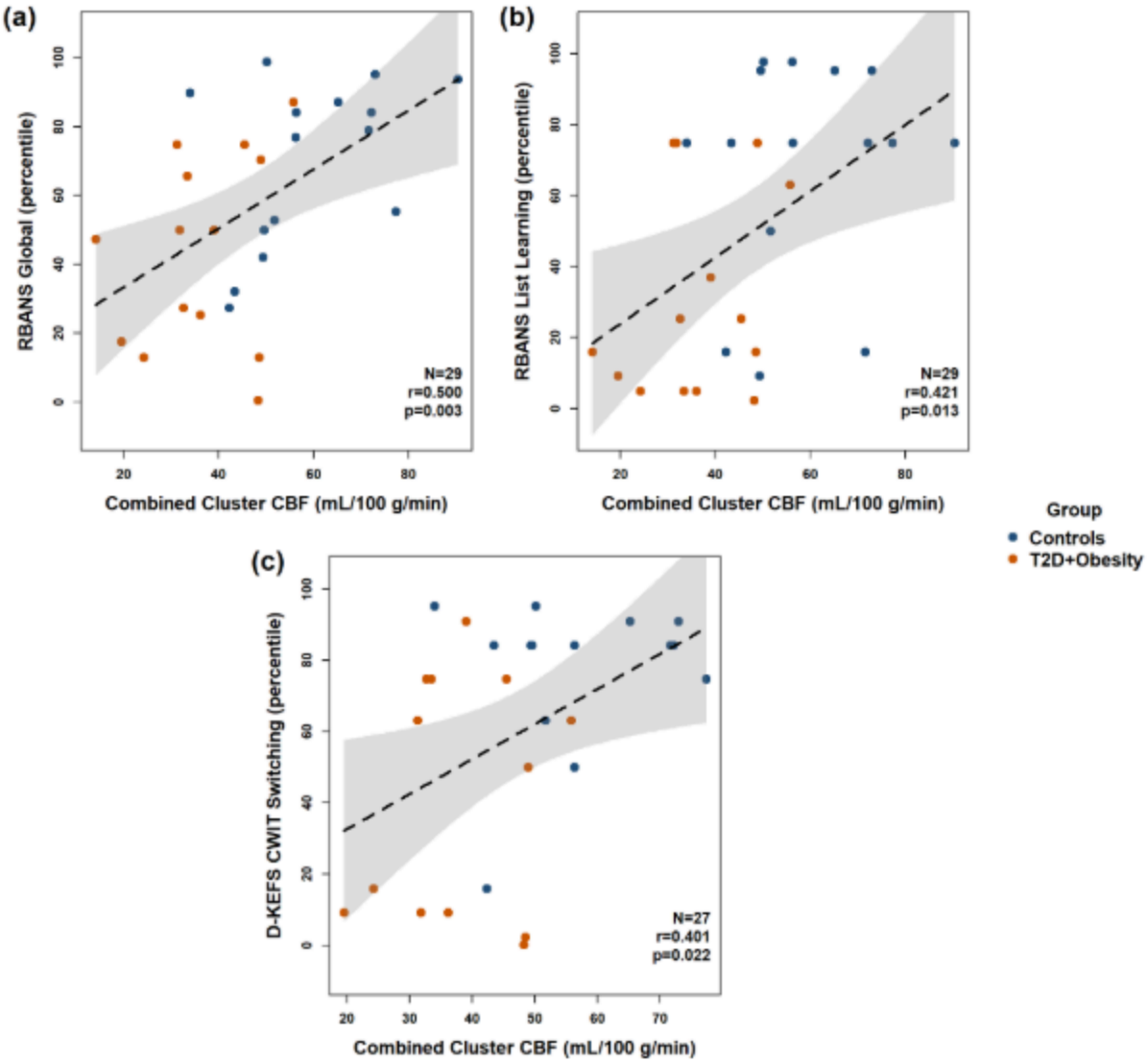


Figure 3

Associations between combined cluster CBF and neuropsychological performance across all participants. Combined cluster CBF was positively associated with (a) RBANS Global (p = 0.003), **(b)** RBANS List Learning (p = 0.013), and **(c)** D-KEFS Switching percentiles (p = 0.022). Note that scatterplots display raw CBF values for visualization, whereas reported statistics were calculated using age-residualized CBF values. Gray color shaded bands represent 95% confidence intervals around the fitted regression line.